Nuclear reaction rates: insights from stellar modeling

Diego Vescovi[1,2]

1. INAF – Osservatorio Astronomico d'Abruzzo, Teramo, Italy
2. INFN – Sezione di Perugia, Perugia, Italy

Finanziato dall'Unione europea NextGenerationEU
Ministero dell'Università e della Ricerca
Italiadomani PIANO NAZIONALE DI RIPRESA E RESILIENZA
INAF ISTITUTO NAZIONALE DI ASTROFISICA Osservatorio Astronomico d'Abruzzo
INFN PERUGIA Istituto Nazionale di Fisica Nucleare Sezione di Perugia

Nucleosynthesis of the heavy elements

Prantzos+ 15, EnAs

- Fusion reactions between charged particles
- Neutron capture processes:
  - **s(low)-process**
  - **i(ntermediate)-process**
  - **r(apid)-process**

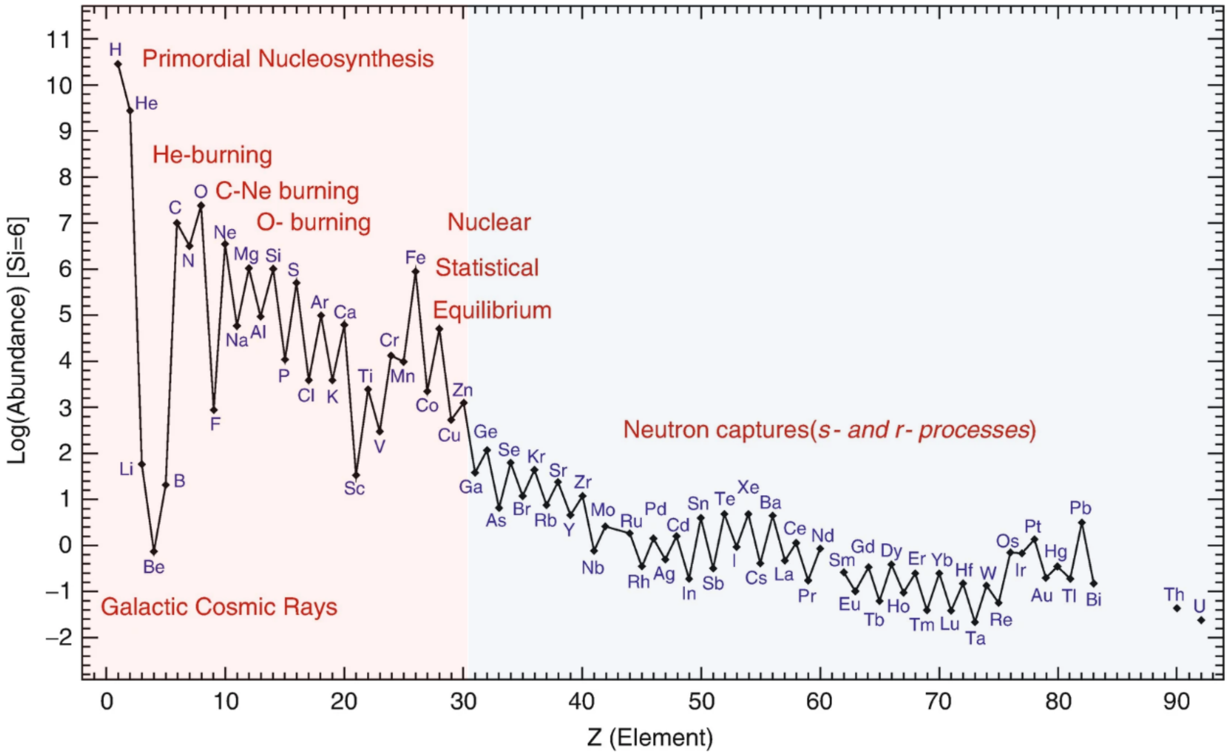

Origin of the heavy elements

s(low) process

- Mild neutron density n_n~10^7
- Asymptotic giant branch (AGB) and massive stars

i(ntermediate) process

- Intemerdiate neutron density n_n~10^{15}
- AGB, rapidly accreting white dwarfs, massive stars, etc.

r(apid) process

- High neutron density $n_n \gtrsim 10^{21}$
- Supernovae and compact binary mergers

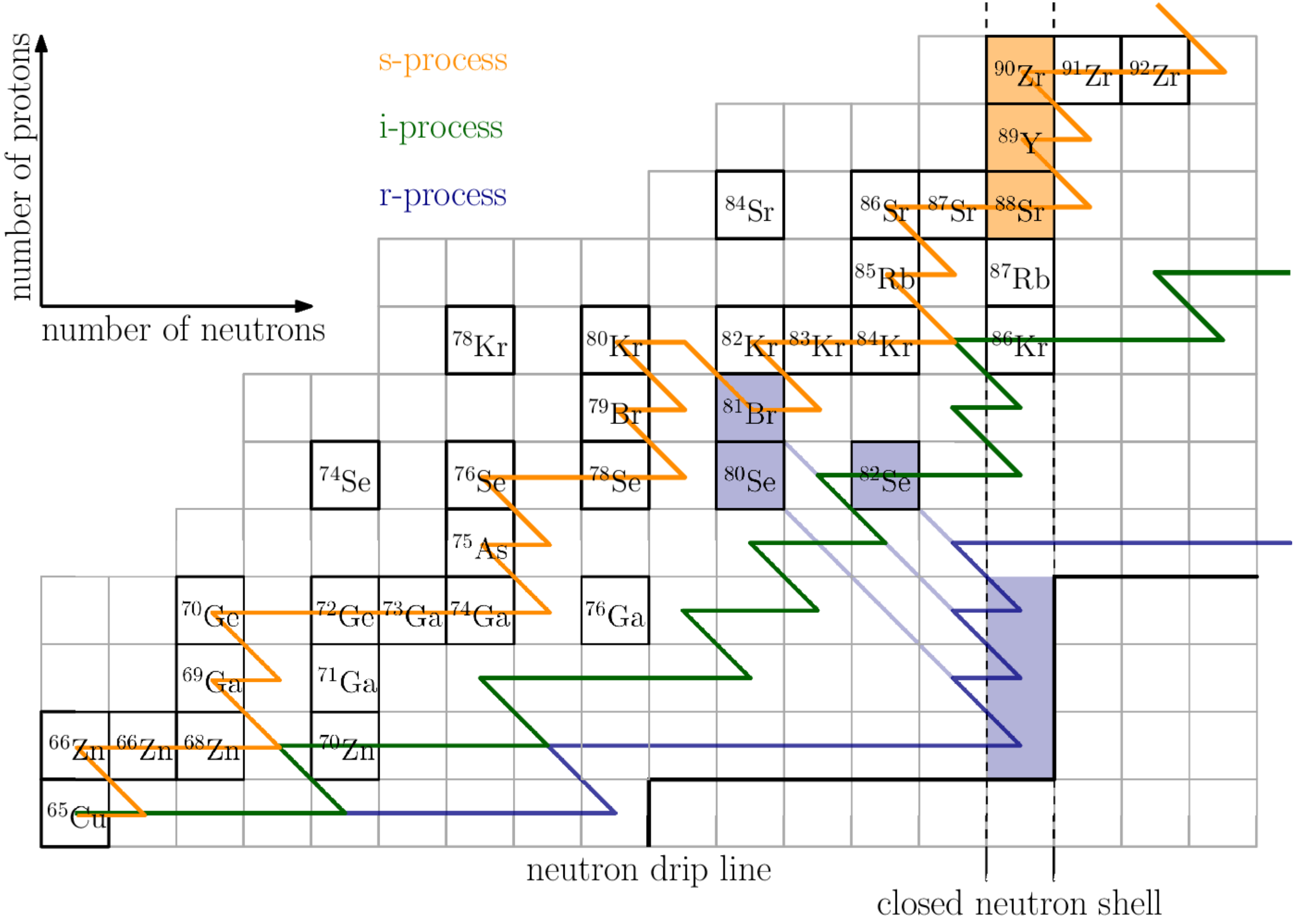

Asymptotic Giant Branch Stars

Straniero+ 06, NuPhA

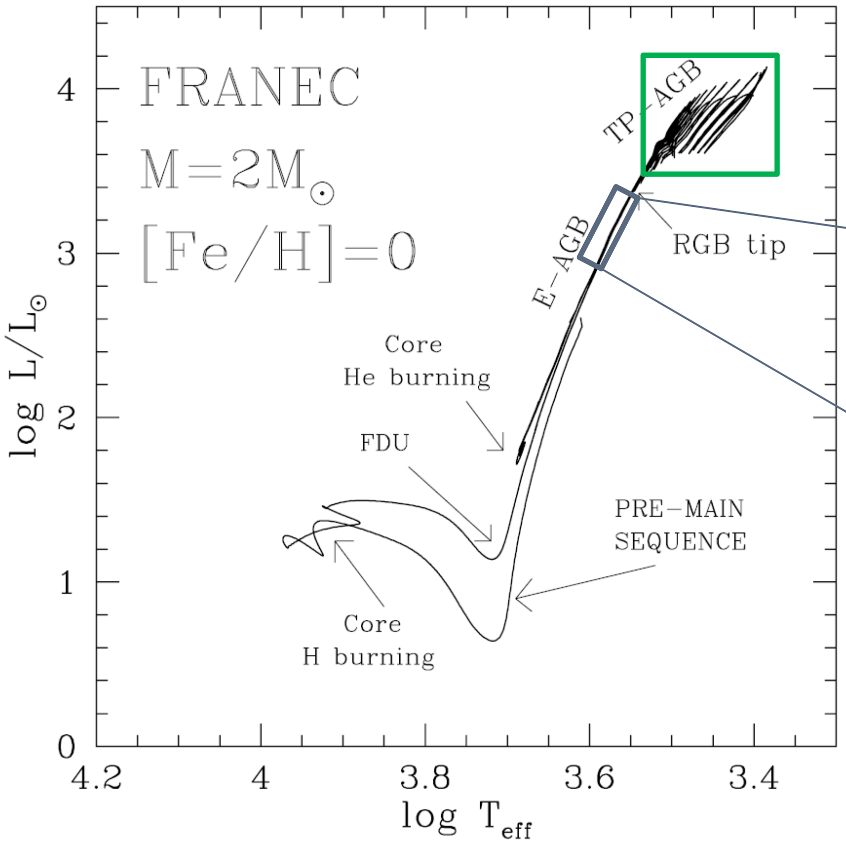

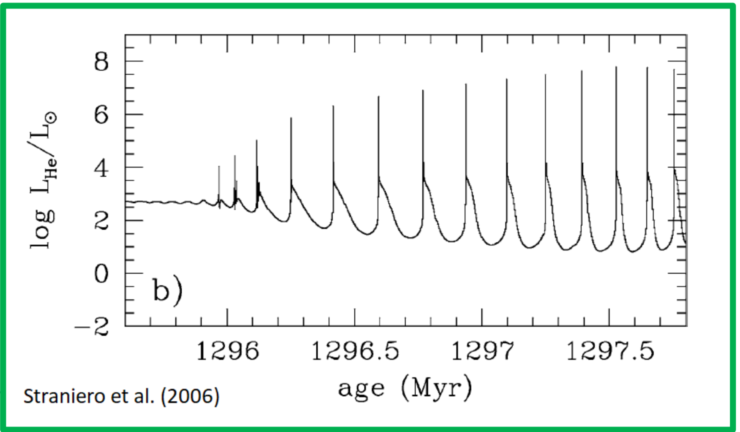

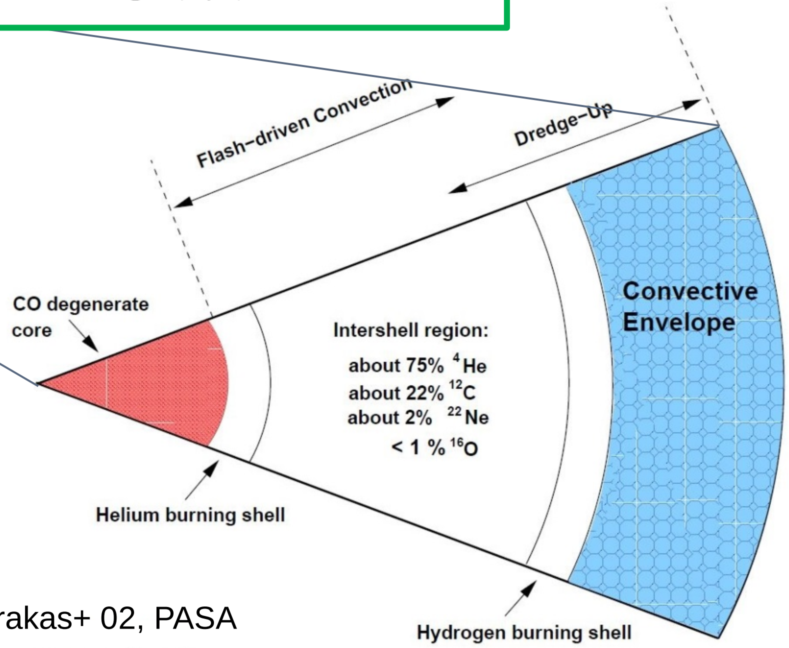

Karakas+ 02, PASA

s-Processing in AGB stars

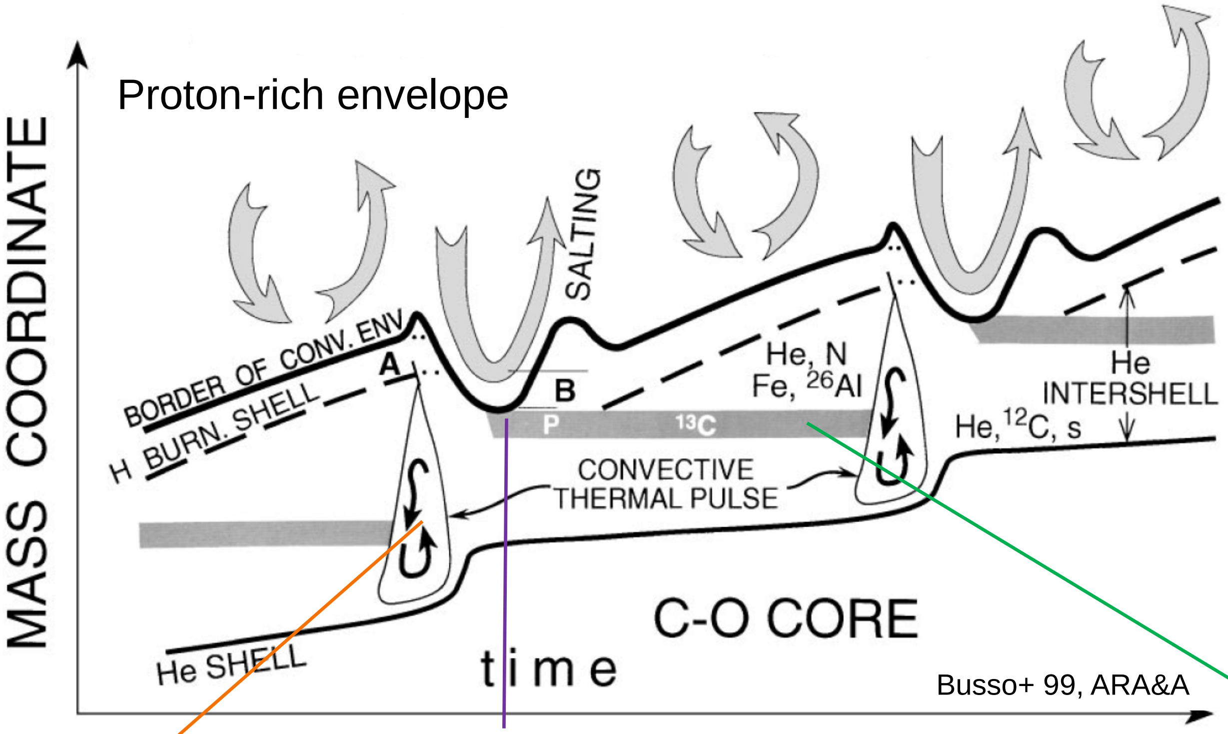

- What?
  Low-Mass Stars
- When?
  Asymptotic Giant Branch (AGB)
- How?
  Thermally Pulsing (TP)

He-flash — Protons — $^{12}C(p,\gamma)^{13}N(\beta^{+}\nu)^{13}C$ — ^{13}C-pocket

$^{22}Ne(\alpha,n)$ —— $^{13}C(\alpha,n)$ ⟶ Heavy elements!!

The formation of the ^{13}C pocket

^{13}C-pocket

^{14}N-pocket

^{14}N strong neutron poison via $^{14}N(n,p)^{14}C$ reaction

Cristallo+ 09, ApJ

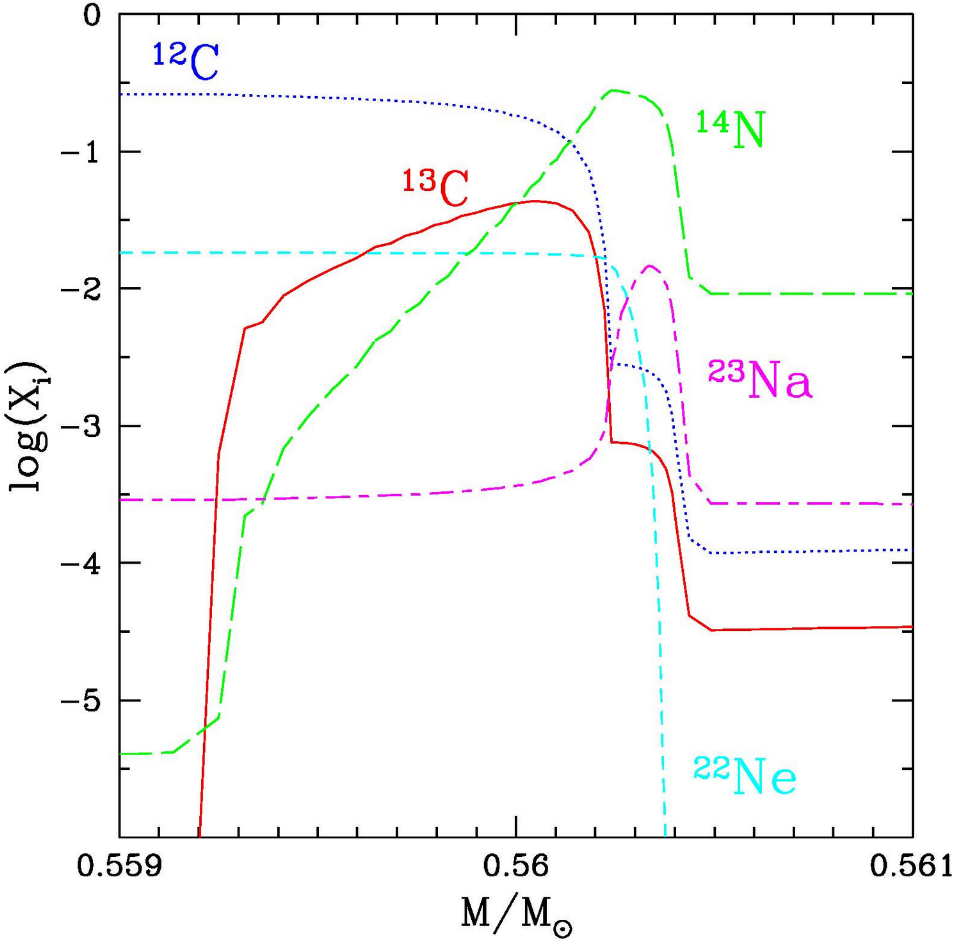

The formation of the ^{13}C pocket

Which is the physical mechanism?

TOP-DOWN MECHANISMS

- Opacity-induced overshoot (Straniero+ 06, Cristallo+ 09, 11, 15)
- Overshoot + internal gravity waves (Battino+ 16, 19, 21)

BOTTOM-UP MECHANISMS

- Magnetic fields (Trippella+ 16; Vescovi+ 20; Busso+ 21)

➡ Magnetic buoyancy

➔ Can change due to **rotationally-induced mixing** (Herwig+ 03; Siess+ 04; Piersanti+ 13)

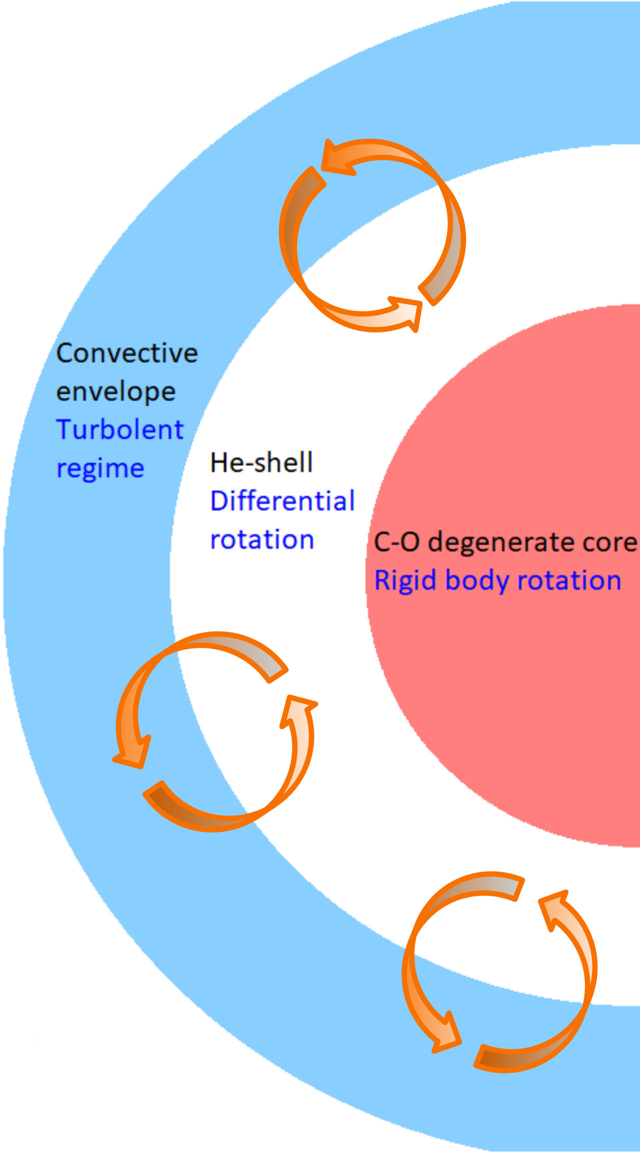

...and outside AGBs?

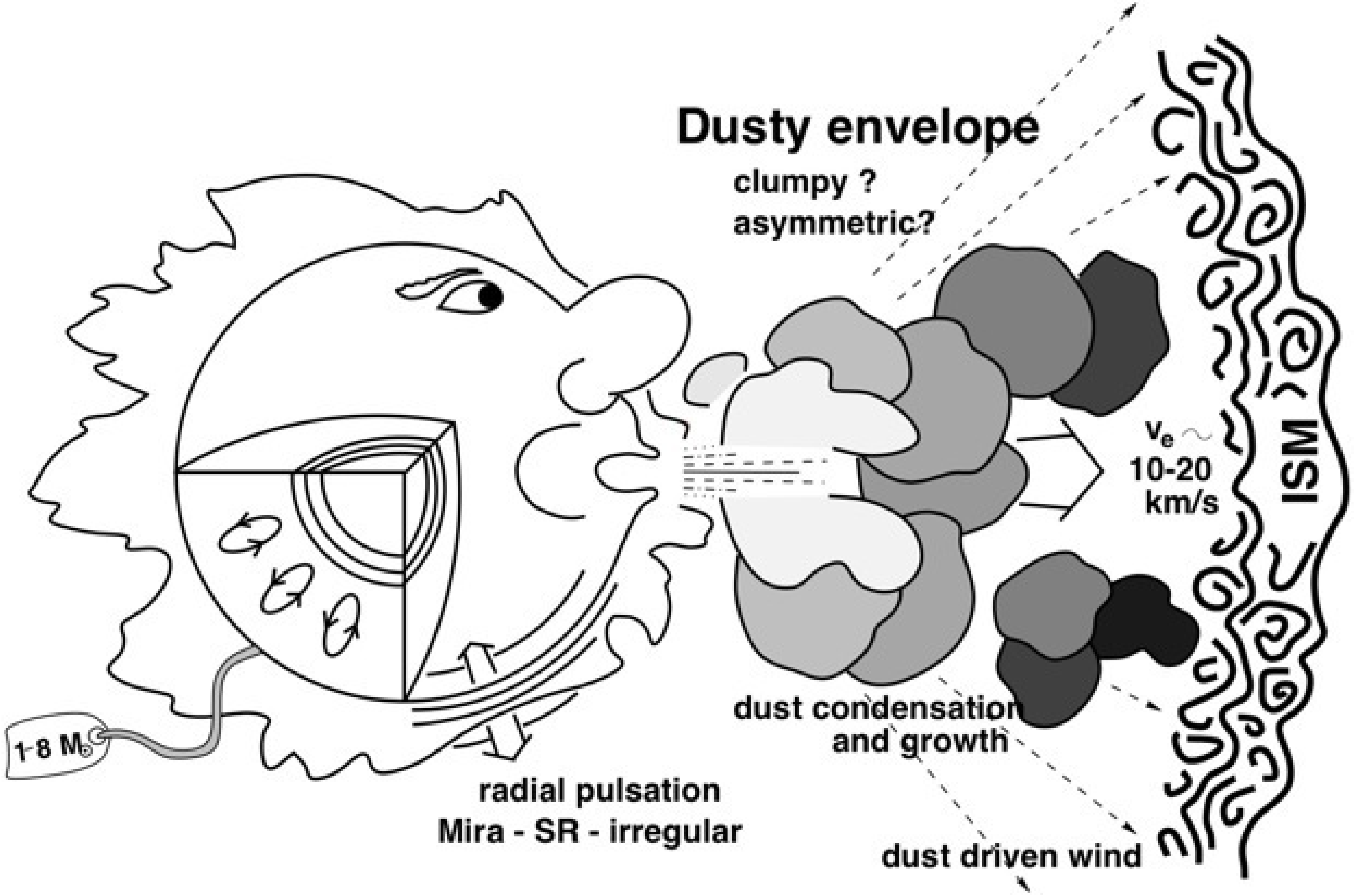

Credit: M. Marengo

AGB stars and presolar SiC grains

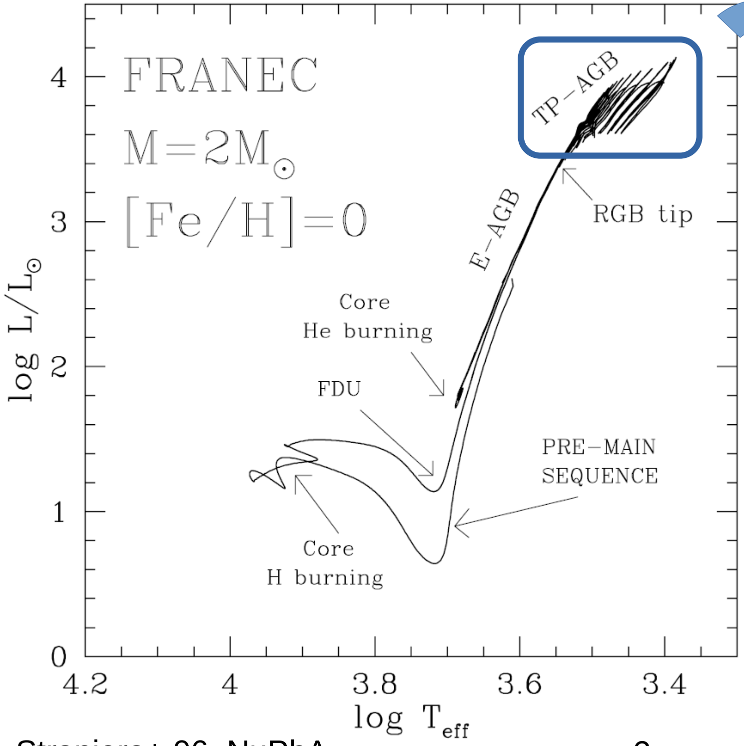

Straniero+ 06, NuPhA

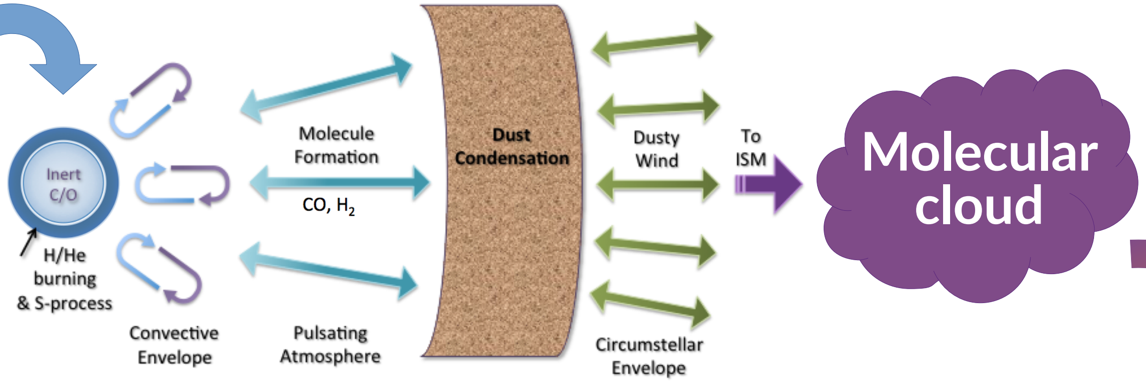

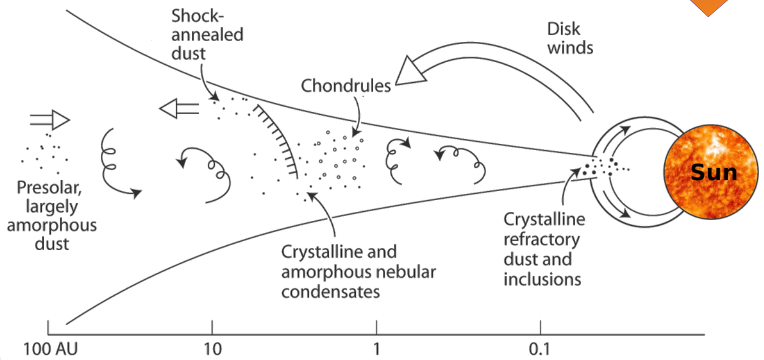

2 µm

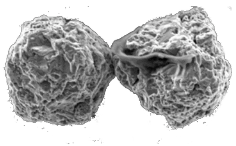

Presolar grains

Meteorites

Constraints to stellar models from presolar SiC grains

Grains can be used to constrain:

1) **Formation of major neutron source ^{13}C**

^{88}Sr/^{86}Sr and ^{138}Ba/^{136}Ba → probe the distribution of ^{13}C pocket

2) **Efficiency of the minor neutron source ^{22}Ne and β−decay rates of branch points**

^{134}Ba/^{136}Ba → ^{134}Cs β^- rate and ^{22}Ne(α,n)^{25}Mg

3) **Neutron-capture cross sections of pure s-isotopes and mixed s,r-isotopes**

^{97}Mo/^{96}Mo → $\sigma(^{96}\mathrm{Mo})_{MACS}/\sigma(^{97}\mathrm{Mo})_{MACS}$

SiC Grains and FRUITY models

- **Isotopic data** including Ni, Sr, Zr, Mo, and Ba isotope ratios in **presolar SiC grains**
- Stellar models with **same initial mass** (2 $M_\odot$) and **solar metallicity**

Vescovi+ 20, ApJL

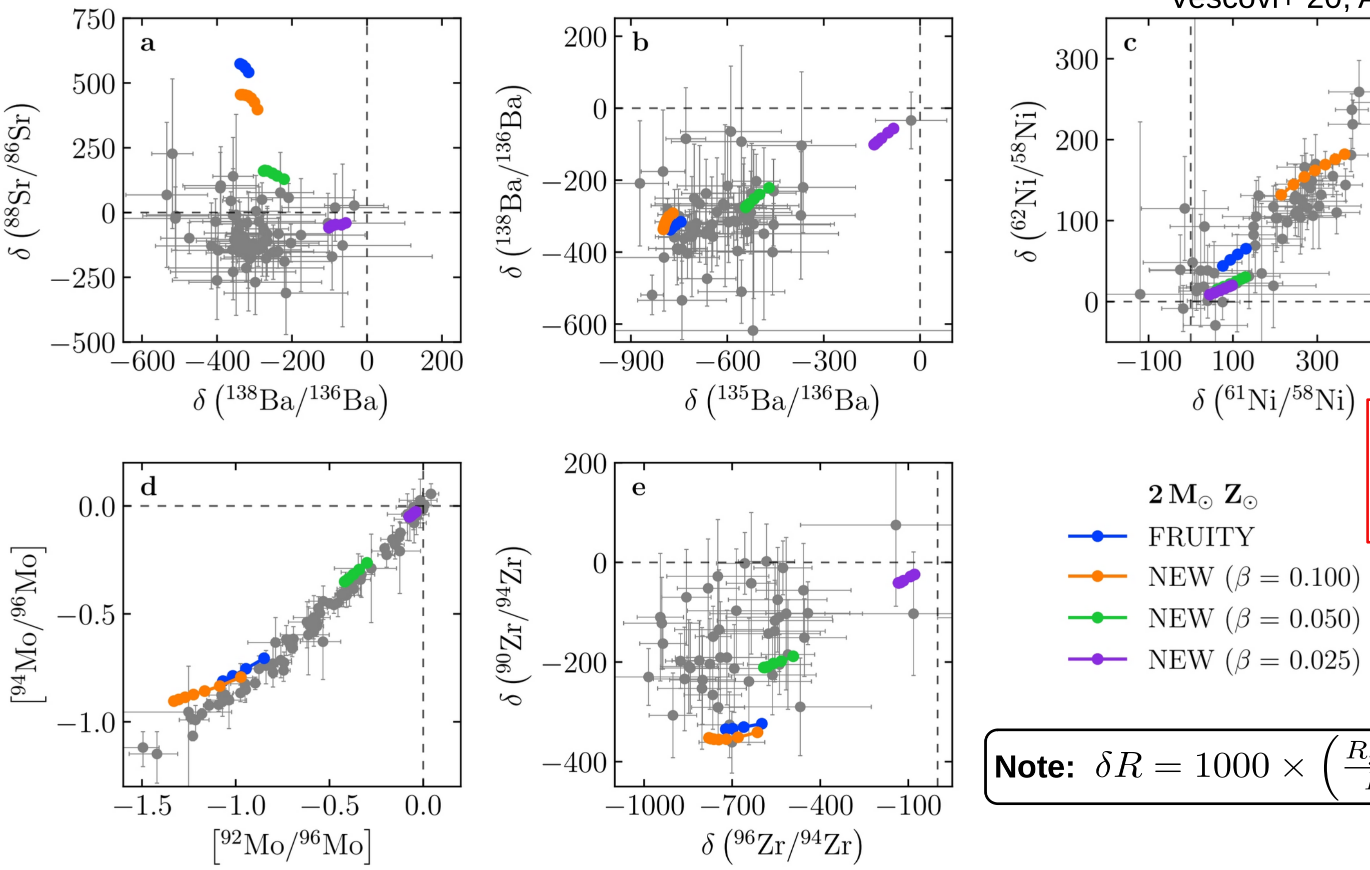

$$v = v_{\rm CE} \exp\left(-\frac{\Delta r}{\beta H_P}\right)$$

Note: $\delta R = 1000 \times \left(\frac{R_{\rm grain}}{R_\odot} - 1\right)$

Magnetic-buoyancy-induced mixing

- **MHD** analytical solutions (Nucci & Busso 14):
- Simple geometry: toroidal magnetic field
- **Magnetic** contribution (Vescovi+ 20) to the dowflow velocity $\boldsymbol{v_d}$, acting when the density distribution is $\rho \propto r^k$:

$$v_d(r) = u_\mathrm{p} \left(\frac{r_\mathrm{p}}{r}\right)^{k+2}$$

  Parameters:
  - Critical toroidal $\boldsymbol{B_\varphi}$

$$B_\varphi \gtrsim \left(4\pi\rho r N^2 H_\mathrm{p} \frac{\eta}{K}\right)^{1/2}$$

  - Starting velocity $\boldsymbol{u_p}$ of the buoyant material

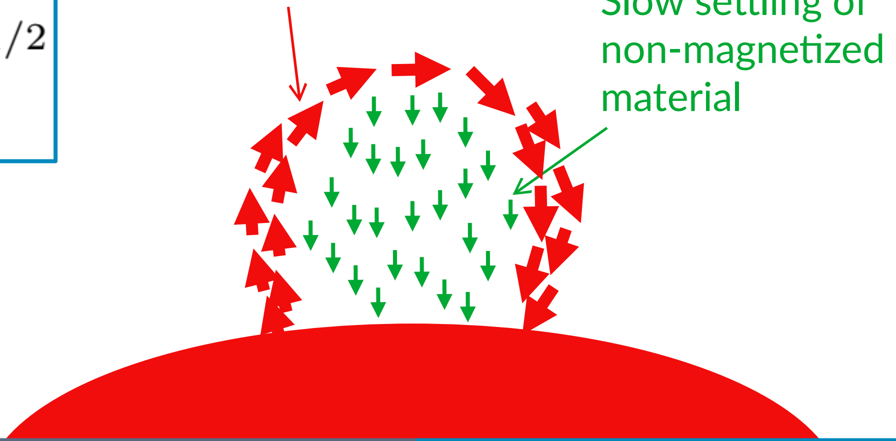

- Calibration is needed!

FRUITY Magnetic: SiC Grains

- Stellar models with **same initial mass** (2 $M_\odot$) and **close-to-solar metallicity**
- **Magnetic** contribution

Vescovi+ 20, ApJL

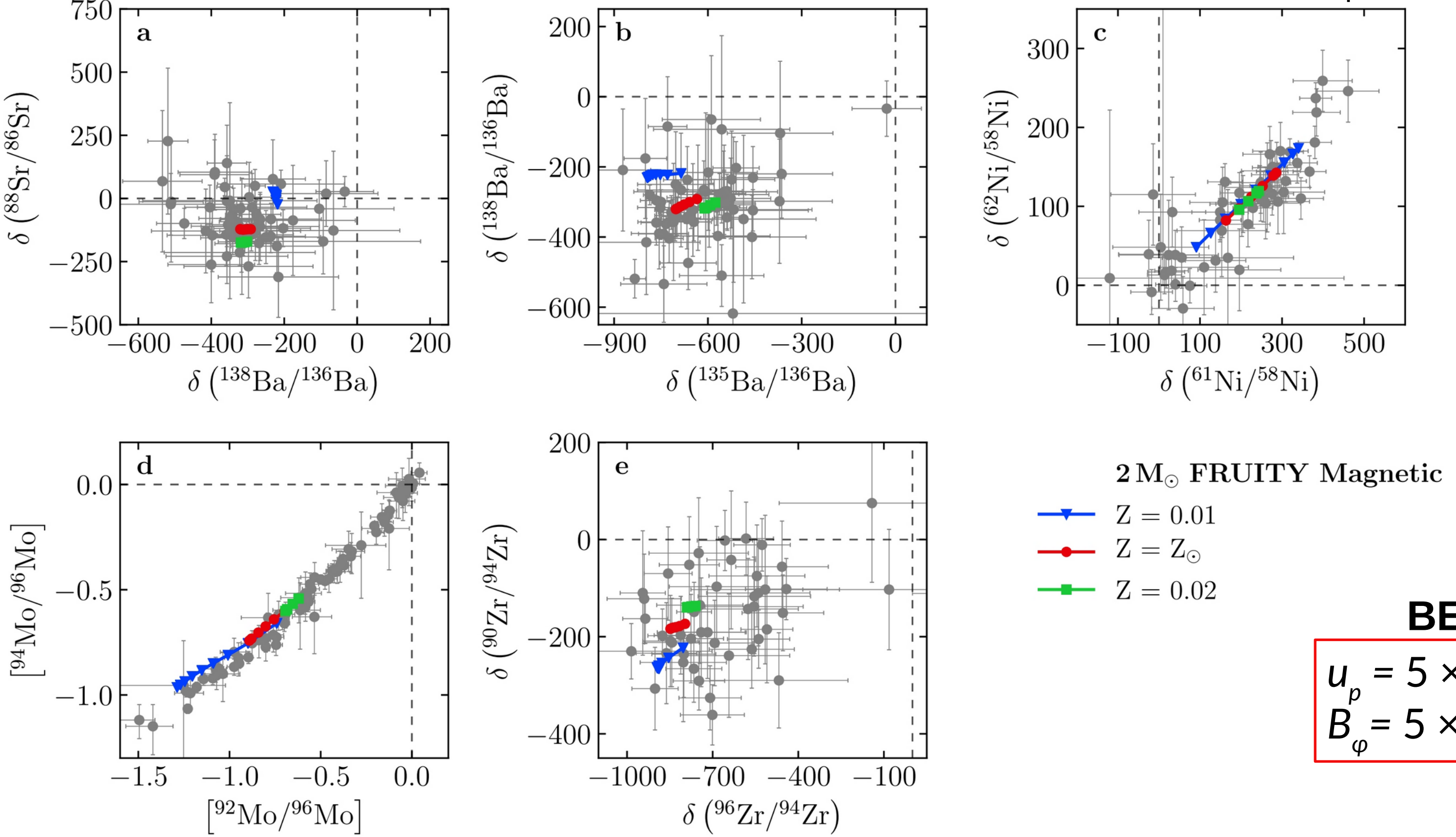

BEST FIT

u_p = 5 × 10^{-5} cm/s
B_φ = 5 × 10^4 G

FRUITY Magnetic: SiC Grains

- **Correlated Sr and Ba isotope analyses** of more MS grains using the new generation of instruments are needed to better quantify the MS grain distribution to determine the data variability, which will help to assess the primary mechanism responsible for the ^{13}C formation
- **Nuclear Experiments**: AGB model predictions for $\delta^{88}Sr$ and $\delta^{138}Ba$ rely directly on the MACS values of ^{86}Sr, ^{88}Sr, ^{136}Ba, and ^{138}Ba
- Current AGB model uncertainties in $\delta^{88}Sr$ and $\delta^{138}Ba$ are controlled by uncertainties in the ^{86}Sr (±10%) and ^{136}Ba (±3%) MACS values, respectively, which correspond to ~200‰ and ~50‰ uncertainties, respectively

→ As the full range of $\delta^{88}Sr$ values observed among MS grains is only ~400‰, new measurements of **^{86}Sr MACS** values are needed to reduce model uncertainties

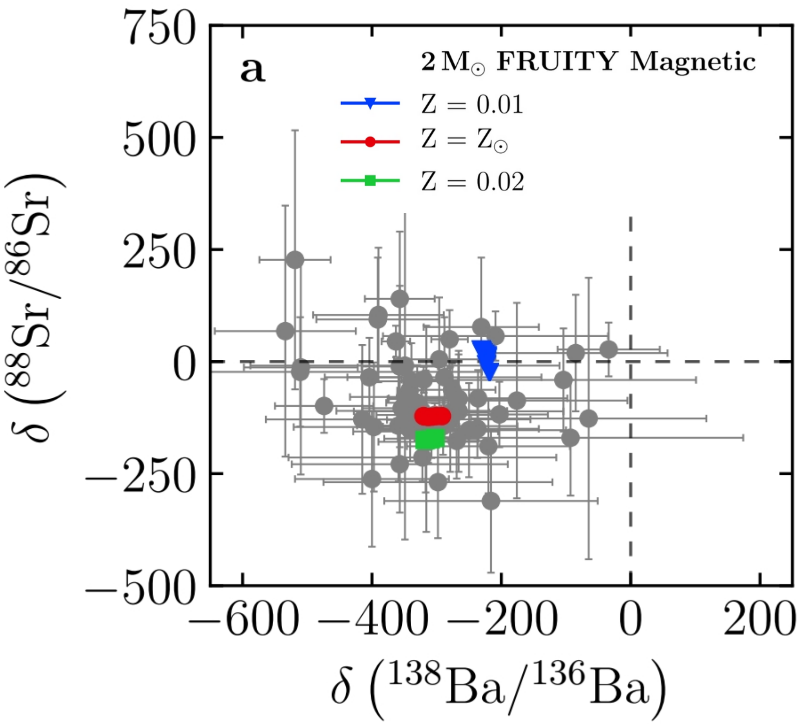

Branchings in the s-process: Cesium isotopes

Bisterzo+ 15, MNRAS

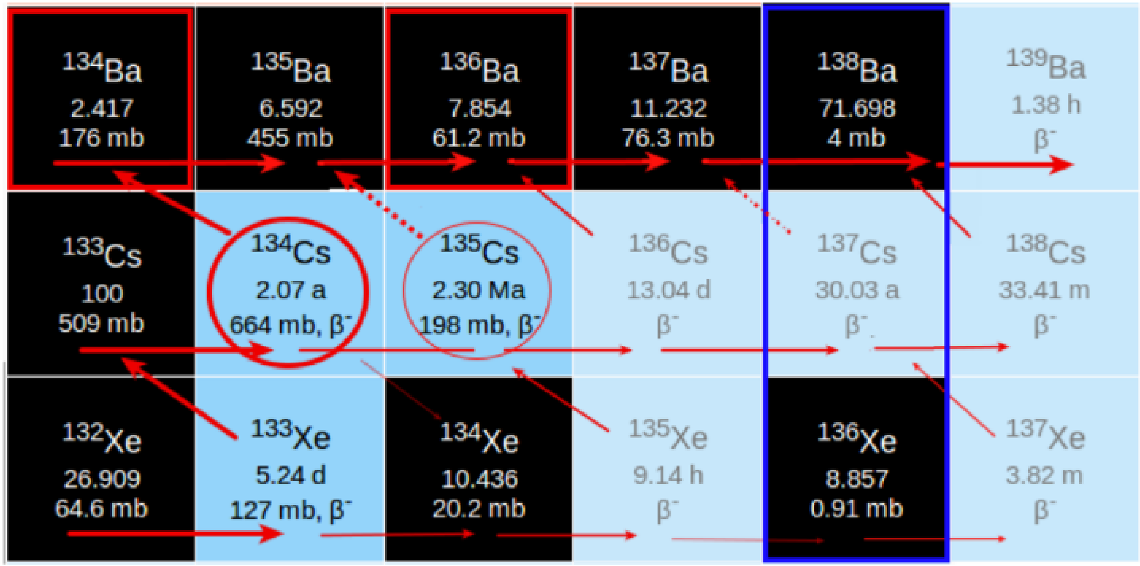

- The chain of branching points at the Cs isotopes is of particular interest not only for understating the ^{135}Cs/^{133}Cs ratio in the Early Solar System

- It affects the isotopic composition of Ba and in particular the relative abundances of the two s-only nuclei **^{134}Ba** and **^{136}Ba** → important for explaining their measured ratio in meteorites (e.g., Busso+ 21, Palmerini+21, Taioli+ 22)

- The half lives of both ^{134}Cs and ^{135}Cs decrease by orders of magnitude in stellar conditions → act as branching point

- The branching point at ^{134}Cs ($T_{1/2}$ = 2 Myr) allows the production of the long-living isotope ^{135}Cs

Branchings in the s-process: Cesium isotopes

- The neutron-capture cross section of ^{135}Cs has been experimentally determined, while the **^{134}Cs(n,γ)** cross section has **only** been **semi-empirically estimated** (Patronis+ 04)

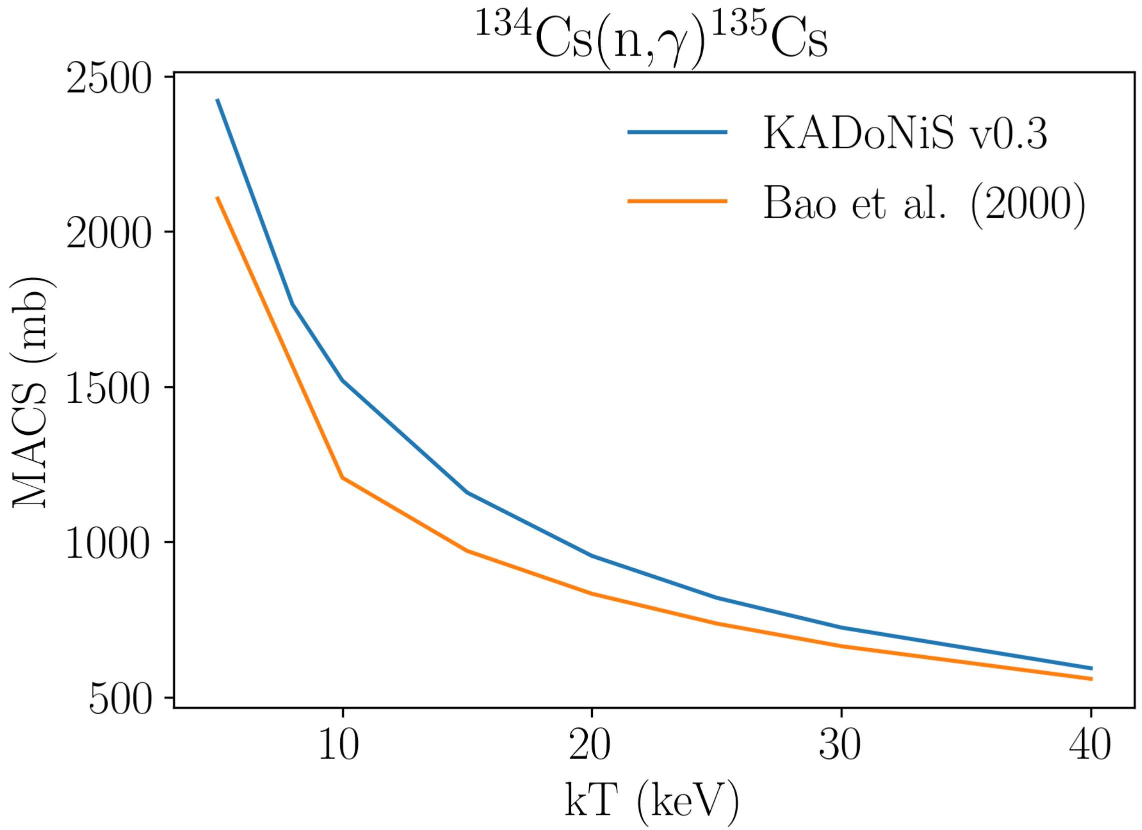

Branchings in the s-process: Cesium isotopes

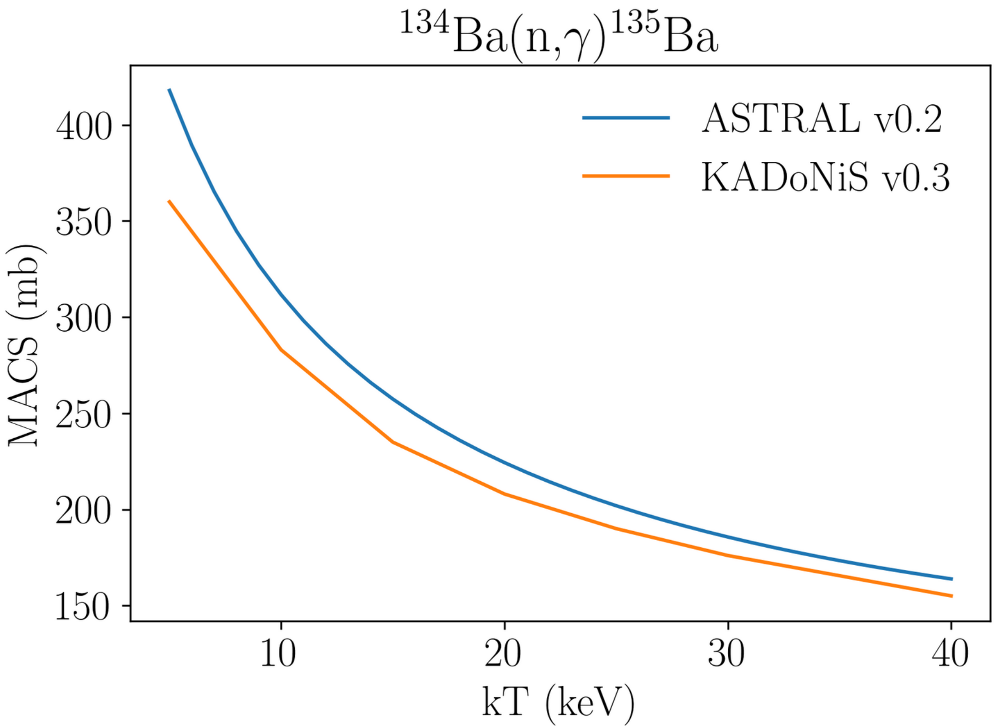

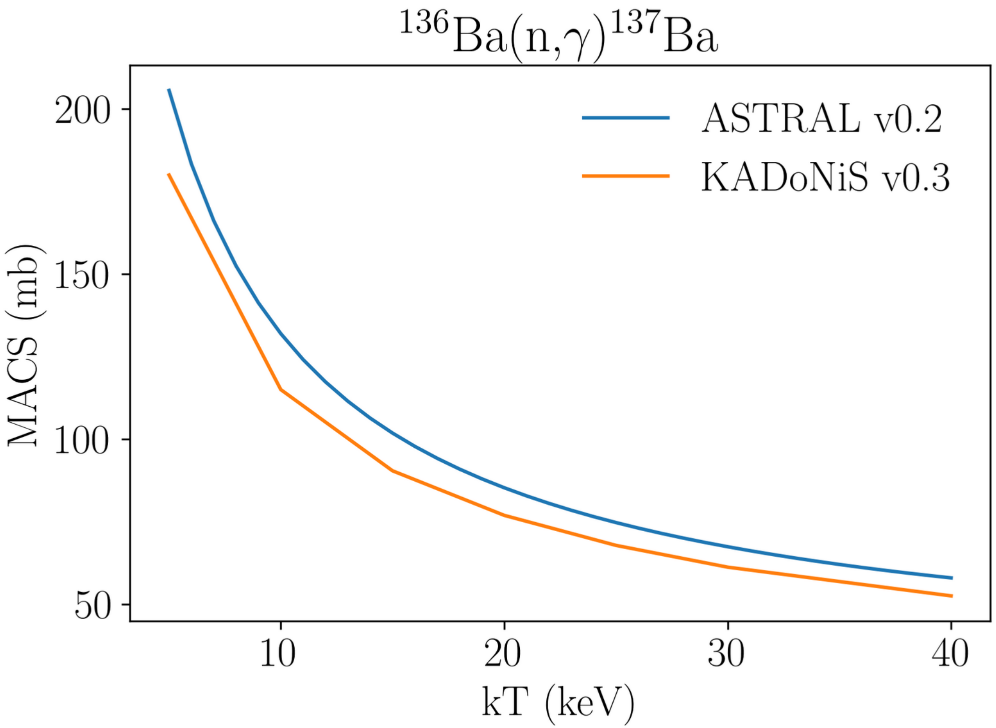

- Re-evaluated cross sections, → systematically higher due to the new (higher by ~5%) adopted gold cross section as a reference

Branchings in the s-process: Cesium isotopes

- $^{22}Ne(\alpha,n)^{25}Mg$ reaction rate uncertain by a **factor ~3**: direct and indirect measurements (e.g., Adsley+21, Shahina+ 24)

- Theoretical ^{134}Cs β^- rate is <u>reduced</u> up to a factor of 8 for $T > 10^8$ K w.r.t Takahashi & Yokoi 87 (Li+ 21, Taioli+ 22)

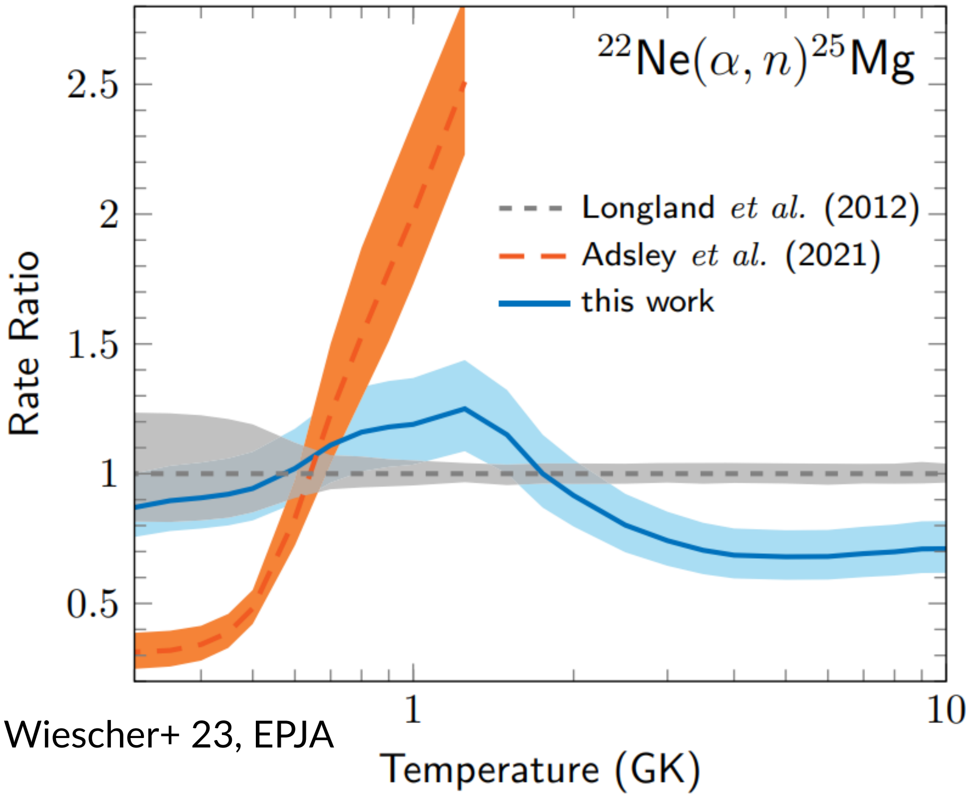

Wiescher+ 23, EPJA

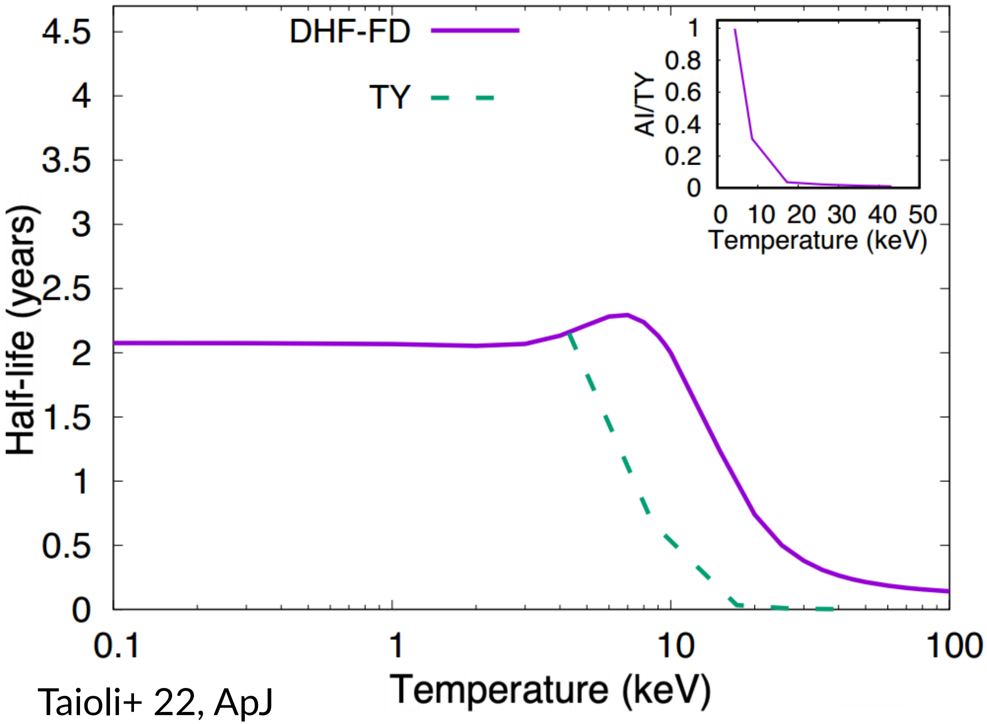

Taioli+ 22, ApJ

Branchings in the s-process: Cesium isotopes

- $^{22}Ne(\alpha,n)^{25}Mg$ reaction rate from Adsley+ 21 with indirect data and with direct data only
- $^{134}Ba(n,\gamma)$ and $^{136}Ba(n,\gamma)$ from ASTRAL v0.2
- ^{134}Cs β^- rate from Takahashi & Yokoi 87 and Taioli+ 22

➔ $^{134}Ba/^{136}Ba$ ratio <u>decreases</u> with enhanced $^{22}Ne(\alpha,n)^{25}Mg$ rate computed from directed data only

➔ $^{134}Ba/^{136}Ba$ ratio <u>decreases</u> with new ^{134}Cs β^- rate

➔ $^{134}Ba/^{136}Ba$ ratio <u>almost unchanged</u> with revised n-capture rates

➔ **Better agreement: Adsley direct + Taioli model**

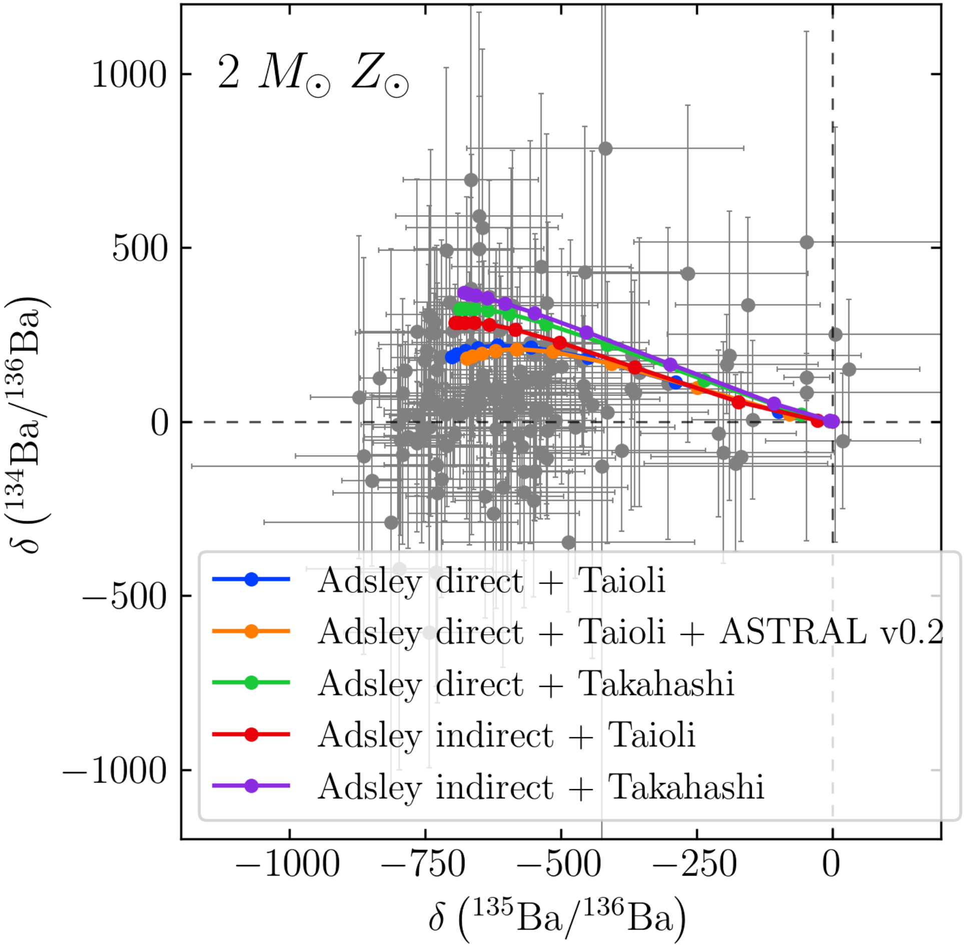

Branchings in the s-process: Cesium isotopes

- Larger stellar masses

→ Higher temperatures during the thermal pulse

→ More efficient $^{22}Ne(\alpha,n)^{25}Mg$ reaction

→ Branching factor $\lambda_\beta/(\lambda_\beta+\lambda_n)$ decreases

- The production of the ^{134}Ba isotope is suppressed

→ **Best agreement: Adsley direct + Taioli models with different stellar masses**

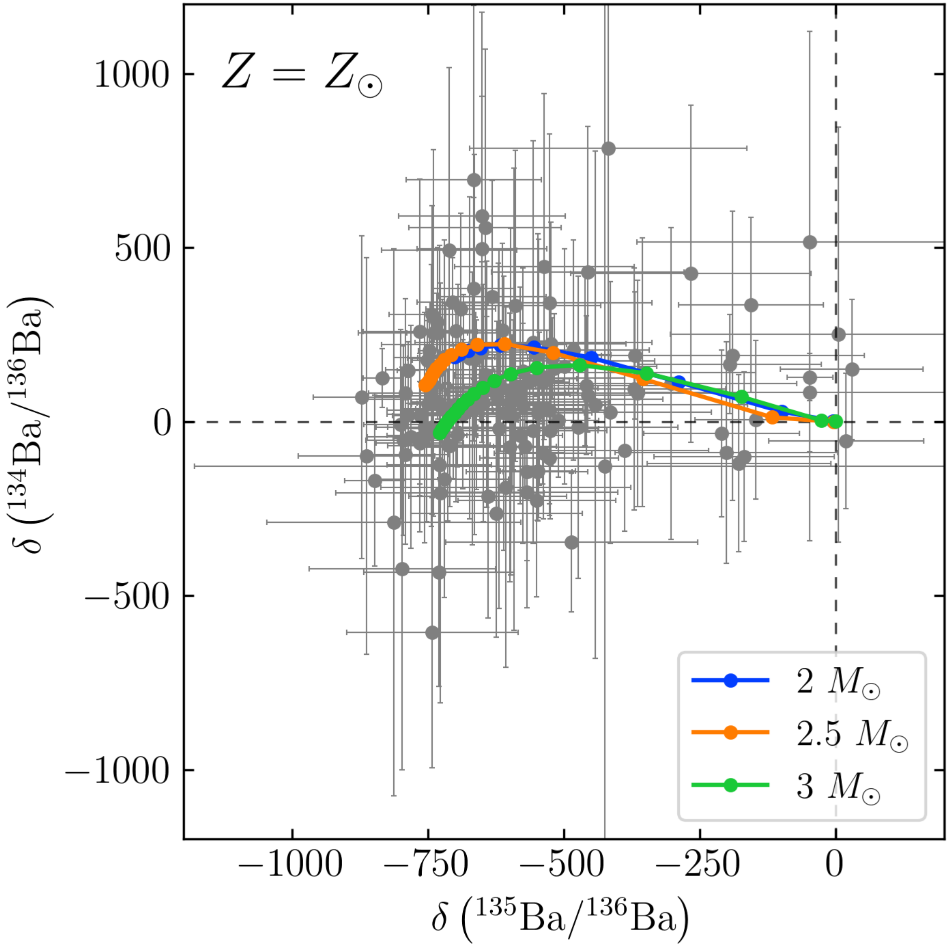

Branchings in the s-process: the case of ^{205}Pb

- Galactic production of **^{205}Pb** is exclusive to the s-process
- It was present in the early Solar System, as testified by meteoritic data
- The ^{205}Pb/^{204}Pb abundance ratio provides us information on the nucleosynthetic events prior to the formation of the Solar System
- Despite its long terrestrial half-life ($T_{1/2}$ = 17 Myr) of **^{205}Pb acts as a branching point** because of the strong dependence on temperature and electron density
- The stable daughter isotope **^{205}Tl becomes unstable during TPs** and its β^- decay is competing with the *e*-capture of ^{205}Pb

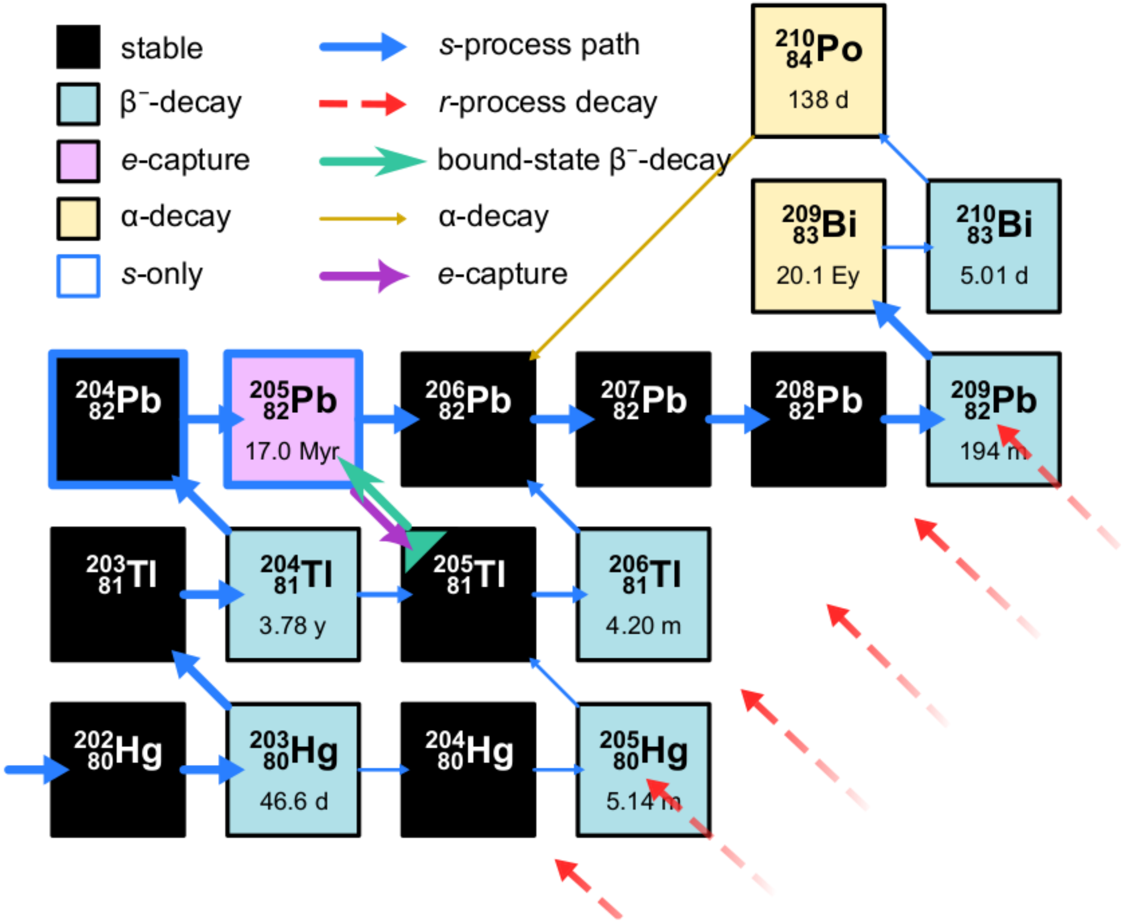

Leckenby+ 24, Nature

Branchings in the s-process: the case of ^{205}Pb

- The weak decay rates of both ^{205}Pb and ^{205}Tl under stellar conditions are determined by the same transition between the spin-1/2 states

- Measuring the half-life in either direction provides us with the nuclear matrix element of the transition → calculate precise astrophysical decay rates

- In the laboratory, measuring the bound-state β−decay of ^{205}Tl is the only way to directly measure the weak nuclear matrix element between the two states

→ **Measured for the first time** the bound-state β^- decay of $^{205}Tl^{81+}$ at GSI

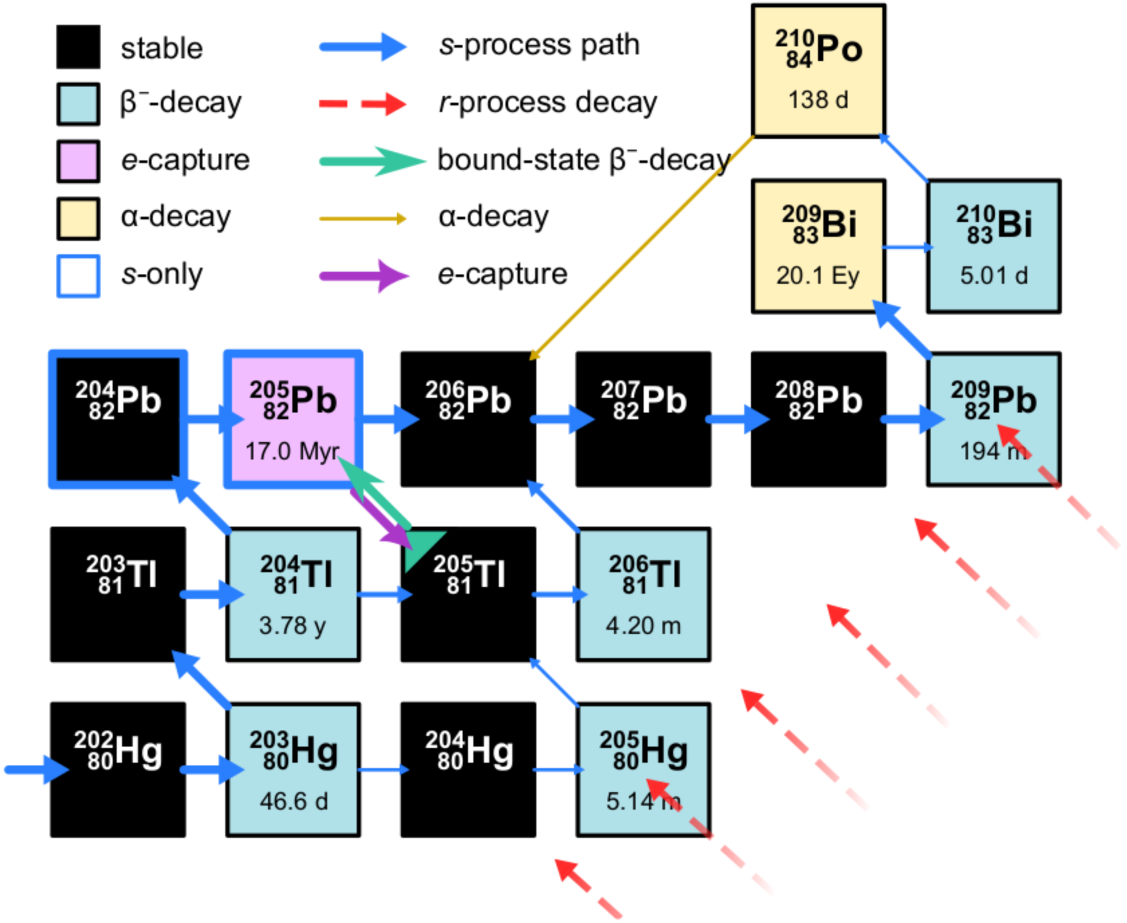

Leckenby+ 24, Nature

Branchings in the s-process: the case of ^{205}Pb

- The new measured half-life is **4.7 times larger** than the previous theoretical estimate (291 days vs. 58 days)
- Reduced decay rates for both the excited-state decay of ^{205}Pb and the bound-state $\beta-$decay of ^{205}Tl
- Calculation of **revised** temperature and density-dependent astrophysical **decay rates** based on a shell-model calculation of all the relevant matrix elements calibrated to the measured rates
- Diverging behavior at low temperatures due to the different extrapolation to the terrestrial value (log versus linear)

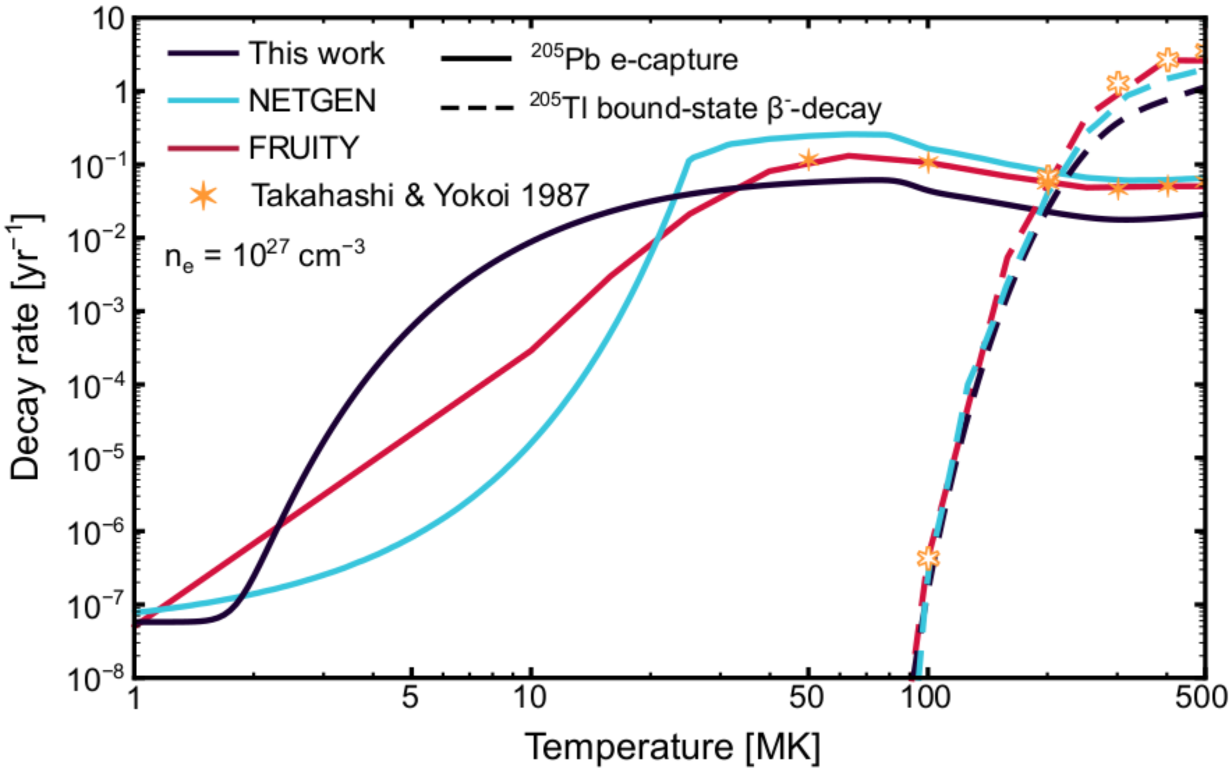

Leckenby+ 24, Nature

Branchings in the s-process: the case of ^{205}Pb

Leckenby+ 24, Nature

- Plugging in new AGB yields in basic GCE models and comparing to the ^{205}Pb/^{204}Pb ratio from meteorites, the isolation time of Solar material inside its parent molecular cloud can be determined

- **Positive isolation times** that are consistent with the other s-process short-lived radioactive nuclei found in the early Solar System

→ However, the **lack of direct experimental data for the ^{205}Pb(n,γ)^{206}Pb** reaction remains a critical limitation for stellar models

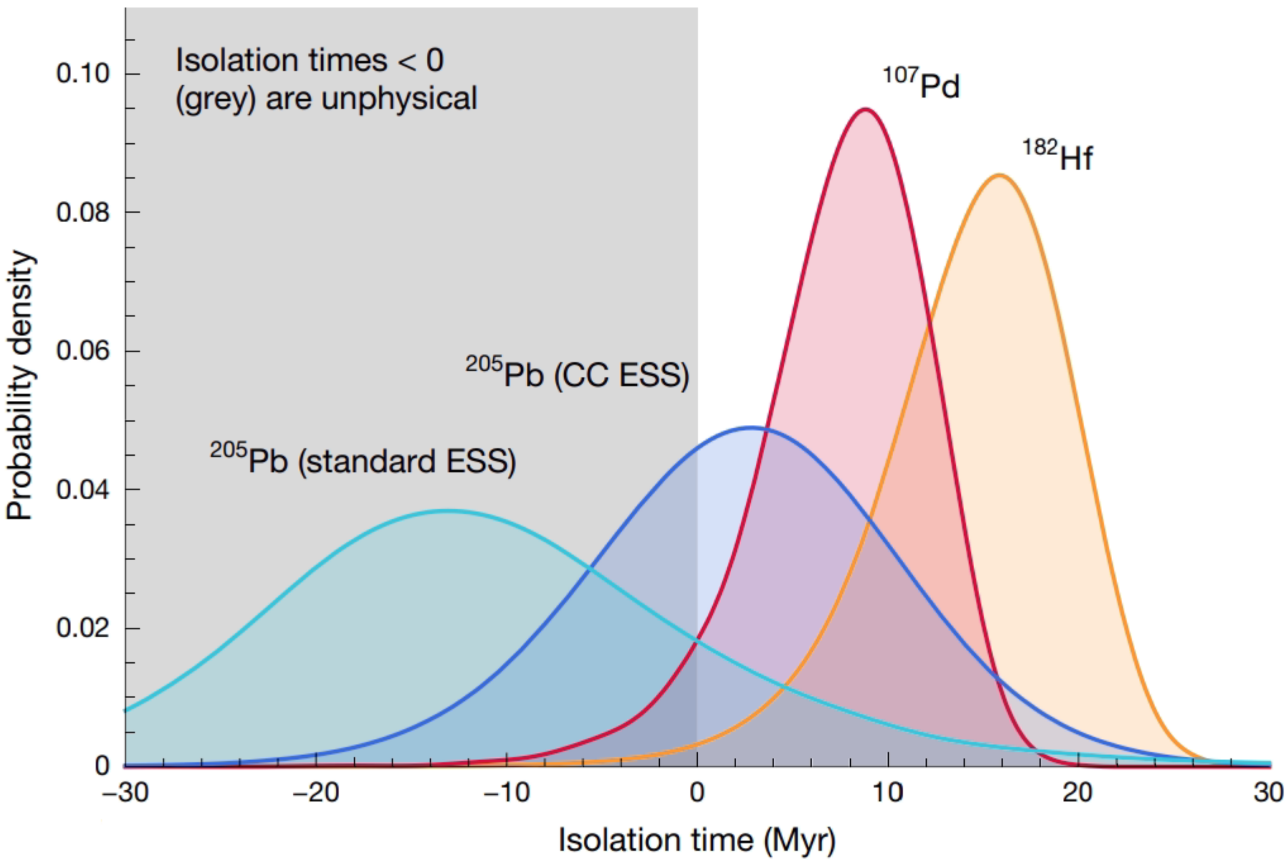

Databases for s-process nucleosynthesis simulations

- Many databases are **old and/or incomplete**
- **Databases for neutron capture reaction rates and decay rates need to be updated and constantly maintained**
- Difficult task, but someone should do it!

NEUTRON CROSS SECTIONS FOR NUCLEOSYNTHESIS STUDIES

Z. Y. BAO,[1] H. BEER, F. KÄPPELER, F. VOSS, and K. WISSHAK

Forschungszentrum Karlsruhe, Institut für Kernphysik
PO Box 3640, D-76021 Karlsruhe, Germany

and

T. RAUSCHER

Institut für Physik, Universität Basel, Klingelbergstrasse 82
CH-4056 Basel, Switzerland

Shell-model calculations of stellar weak interaction rates: II. Weak rates for nuclei in the mass range $A = 45{-}65$ in supernovae environments

K. Langanke and G. Martínez-Pinedo

Institut for Fysik og Astronomi, Århus Universitet, DK-8000 Århus C, Denmark

Received 20 December 1999; revised 27 January 2000; accepted 28 January 2000

BETA-DECAY RATES OF HIGHLY IONIZED HEAVY ATOMS IN STELLAR INTERIORS*

K. TAKAHASHI

University of California, Institute of Geophysics and Planetary Physics
Lawrence Livermore National Laboratory, Livermore, California 94550

and

K. YOKOI†

Kernforschungszentrum Karlsruhe GmbH, Institut für Kernphysik III
D-7500 Karlsruhe, Federal Republic of Germany

Nucleosynthesis in Stars • Karlsruhe Astrophysical Database of Nucleosynthesis in Stars 0.3

The new version KADoNiS v0.3 is finally online!

Version 0.3 provides data for 357 isotopes including 5 newly added isotopes, 42 updated MACS30, new stellar enhancement factors, and the MACS30 obtained from three different evaluated data libraries. More information below or in the logbook.

NetGen
NUCLEAR NETWORK GENERATOR

ASTRAL

ASTrophysical Rate and rAw data Library

Backup slides

Branchings in the s-process

- During the s-process, radioactive nuclei act as branching points on the path of neutron captures, generating a huge diversity of possibilities in the production of the isotopes up to Bi

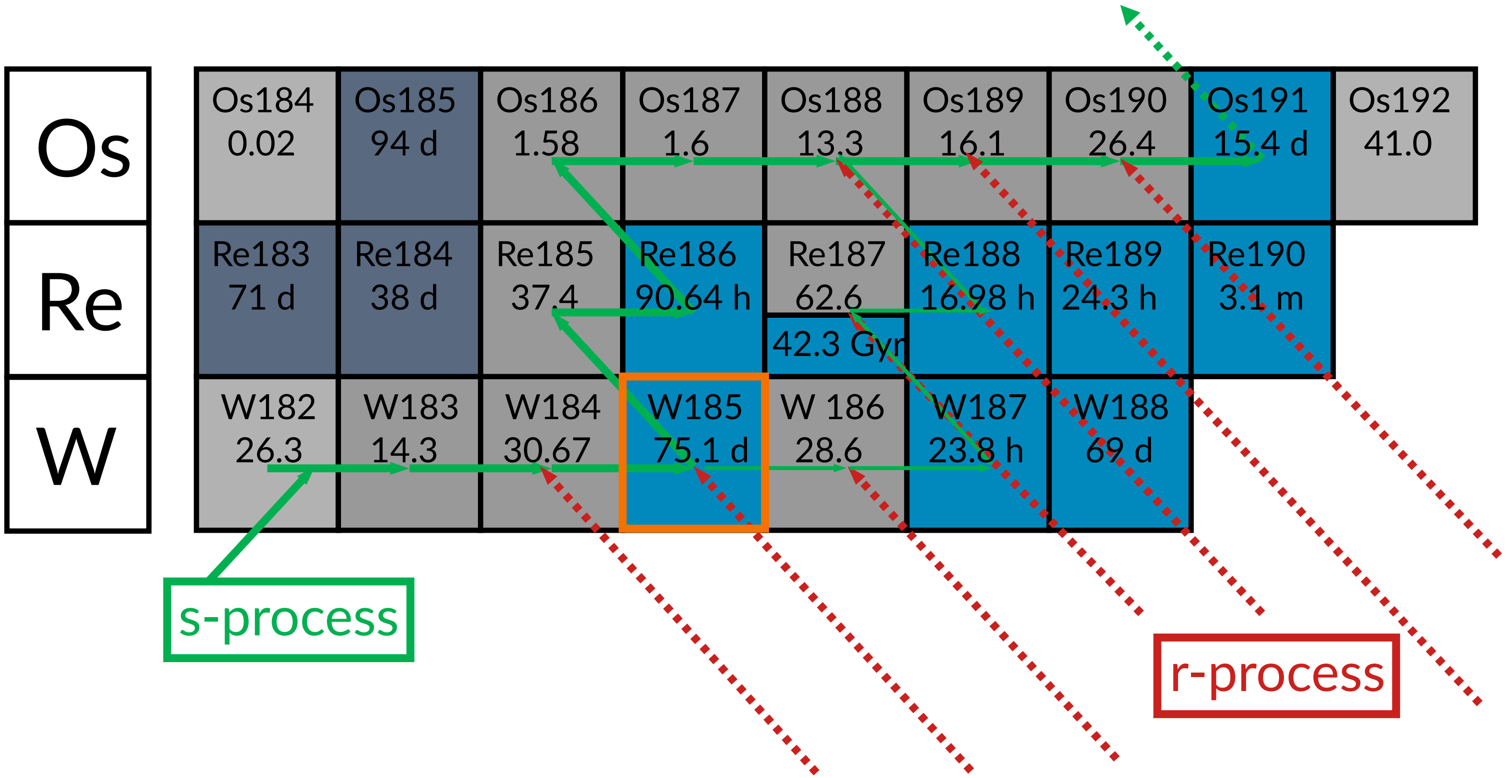

- **Branching points**: if $\tau_n \sim \tau_\beta$ several paths are possible

The Early Solar System

Lugaro+ 18, PrPNP

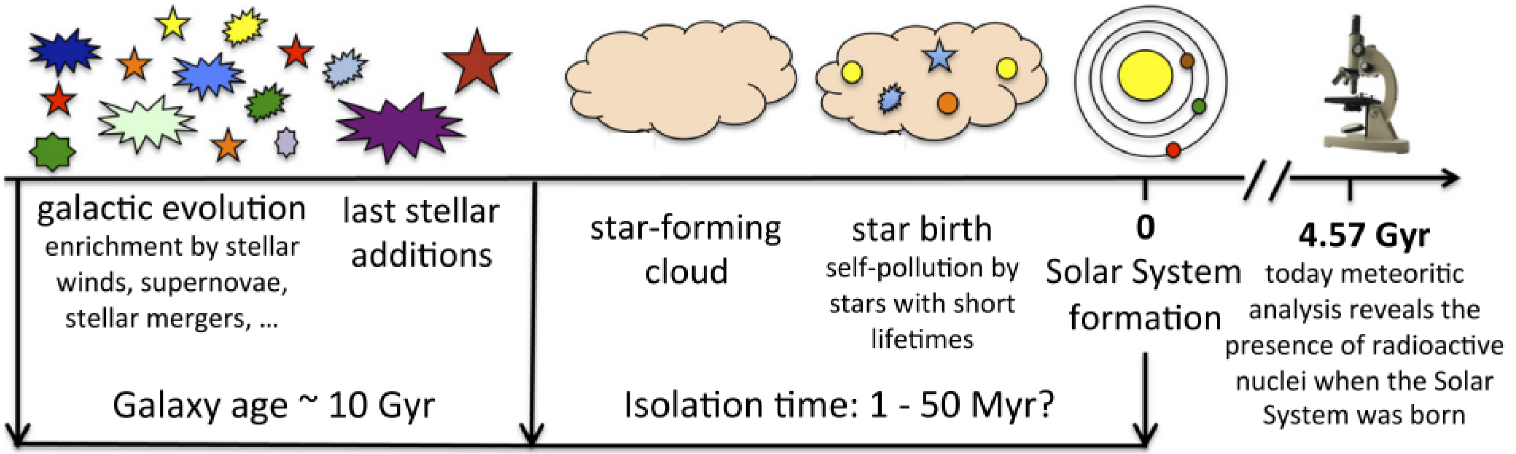

- Some of these radionuclides were present in the first few million years of Solar System history
- Their presence is inferred through excesses in daughter isotopes (compared to normal terrestrial isotopic composition) in various materials found in primitive meteorites
- Their abundances have profound impact on the timing of stellar nucleosynthesis events prior to Solar System formation, chronology of events in the early Solar System, early solar activity, heating of early-formed planetesimals, and chronology of planet formation

The Early Solar System

- The survival of ^{135}**Cs** and ^{205}**Pb** in stellar environments is very uncertain because of the strong temperature and density dependence of their half lives, decreasing by orders of magnitudes in stellar conditions and determined only theoretically

- ^{107}**Pd** and ^{205}**Pb** are produced by neutron captures on the stable isotopes

- ^{135}**Cs** and ^{182}**Hf** can be reached via the activation of branching points at ^{134}**Cs** and ^{181}**Hf**, respectively

Table 1 SLRs once existing in Solar System objects; shaded rows indicate SLRs with unconfirmed or uncertain abundances

Davis A. M. 22, ARA&A

Fractionation[a]	Parent nuclide	Half-life (Ma)[b]	Daughter nuclide	Estimated initial Solar System abundance	Objects found in	Reference(s)
Nebular	^{7}Be	53.22 ± 0.06 d	^{7}Li	$(6.1 \pm 1.3) \times 10^{-3} \times {}^{9}$Be	CAI	27
Nebular	^{10}Be	1.387 ± 0.0012	^{10}B	$(7.3 \pm 1.7) \times 10^{-4} \times {}^{9}$Be	CAIs	36; this article
Nebular, planetary	^{26}Al	0.717 ± 0.024	^{26}Mg	$(5.20 \pm 0.13) \times 10^{-5} \times {}^{27}$Al	CAIs, chondrules, achondrites	44, 45
Planetary	^{36}Cl	0.3013 ± 0.0015	^{36}S, ^{36}Ar	$(1.7\text{–}3.0) \times 10^{-5} \times {}^{35}$Cl	CAIs, chondrites	55
Nebular	^{41}Ca	0.0994 ± 0.0015	^{41}K	$4 \times 10^{-9} \times {}^{40}$Ca	CAIs	62
Nebular, planetary	^{53}Mn	3.7 ± 0.4	^{53}Cr	$(7 \pm 1) \times 10^{-6} \times {}^{55}$Mn	CAIs, chondrules, carbonates, achondrites	69
Nebular, planetary	^{60}Fe	2.62 ± 0.04	^{60}Ni	$(1.01 \pm 0.27) \times 10^{-8} \times {}^{56}$Fe	Achondrites, chondrites	79
Planetary	^{92}Nb	34.7 ± 2.4	^{92}Zr	$(1.66 \pm 0.10) \times 10^{-5} \times {}^{93}$Nb	Chondrites, mesosiderites	89
Planetary	^{97}Tc	4.21 ± 0.16	^{97}Mo	$<1 \times 10^{-6} \times {}^{92}$Mo	Iron meteorites	90
Planetary	^{98}Tc	4.2 ± 0.3	^{98}Ru	$<2 \times 10^{-5} \times {}^{96}$Ru	Iron meteorites	91
Planetary	^{107}Pd	6.5 ± 0.3	^{107}Ag	$(5.9 \pm 2.2) \times 10^{-5} \times {}^{108}$Pd	Iron meteorites, pallasites	94
Planetary	^{126}Sn	0.230 ± 0.014	^{126}Te	$<3 \times 10^{-6} \times {}^{124}$Sn	Chondrules, secondary minerals	101
Planetary	^{129}I	16.14 ± 0.12	^{129}Xe	$(1.35 \pm 0.02) \times 10^{-4} \times {}^{127}$I	Chondrules, secondary minerals	This article
Nebular	^{135}Cs	1.33 ± 0.19	^{135}Ba	$<2.8 \times 10^{-6} \times {}^{133}$Cs	CAIs, chondrites	109
Planetary	^{146}Sm	103 ± 5[c]	^{142}Nd	$(8.40 \pm 0.32) \times 10^{-3} \times {}^{144}$Sm	Planetary differentiates	114
Planetary	^{182}Hf	8.90 ± 0.09	^{182}W	$(1.018 \pm 0.043) \times 10^{-4} \times {}^{180}$Hf	CAIs, planetary differentiates	117
Planetary	^{205}Pb	17.0 ± 0.9	^{205}Tl	$(1.8 \pm 1.2) \times 10^{-3} \times {}^{204}$Pb	Chondrites	121
Planetary	^{244}Pu	81.3 ± 0.3	^{232}Th; fission	$(7.7 \pm 0.6) \times 10^{-3} \times {}^{238}$U	CAIs, chondrites	123
Nebular	^{247}Cm	15.6 ± 0.5	^{235}U	$(5.6 \pm 0.3) \times 10^{-3} \times {}^{235}$U	CAIs	4, 55

Branchings in the s-process: the case of ^{205}Pb

- The <u>bulk of ^{205}Pb is produced during TPs</u>

- During the phase between the end of each TP and the start of the following dredge-up, **^{205}Pb decays** according to the local temperature and electron density, whilst **^{205}Tl decay** doesn't

- Once carried to the convective envelope the ^{205}Pb abundance is <u>preserved and ejected</u> in the interstellar medium via stellar winds

- NEW/FRUITY(TY87) → ^{205}Pb/^{204}Pb ratio **decreased** of a factor ~4

- NEW/NETGEN → ^{205}Pb/^{204}Pb ratio **increased** of a factor ~7

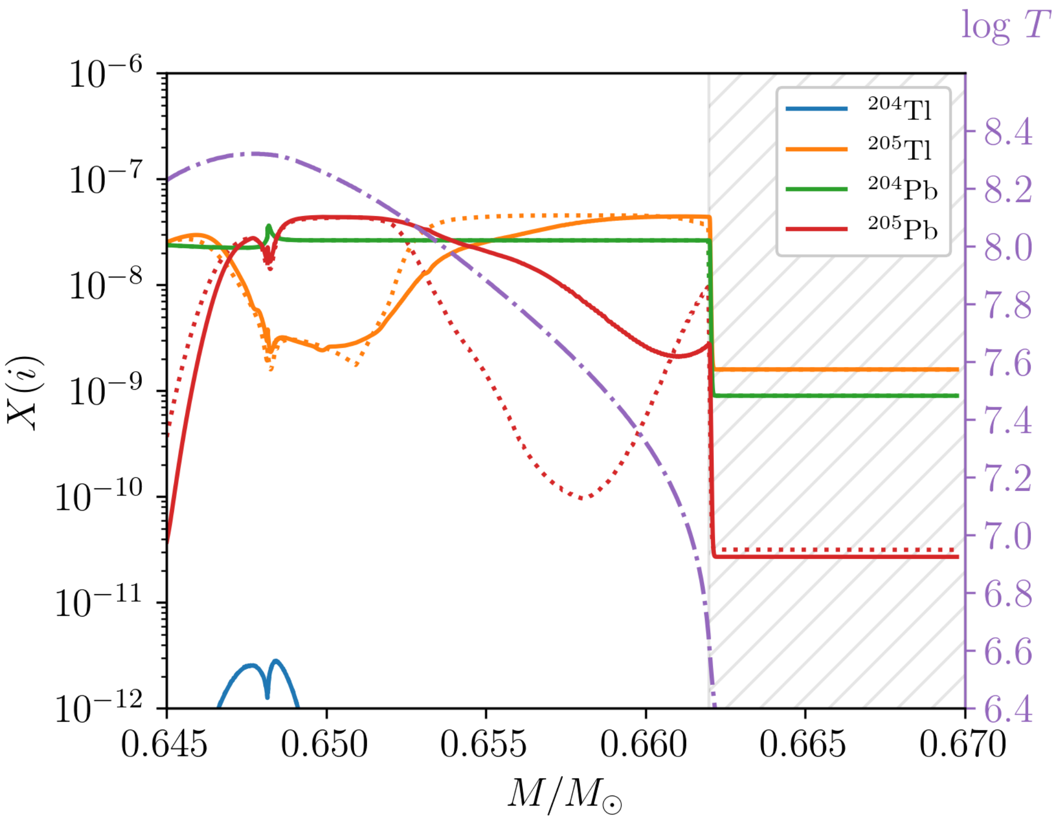

Neutron poisons: the case of ^{22}Ne

- Primary ^{12}C is produced by partial He burning in the pulse and is mixed with the shell by previous third dredge-up episodes

- The H shell converts all CNO nuclei to ^{14}N, which is then converted to ^{22}Ne by double α capture during the early development of the next thermal instability

- A very large abundance of primary ^{22}Ne is present in the pulse

- For lower metallicities the importance of ^{22}Ne as a neutron poison increases strongly

- For higher metallicities the impact of primary ^{22}Ne is strongly diminished

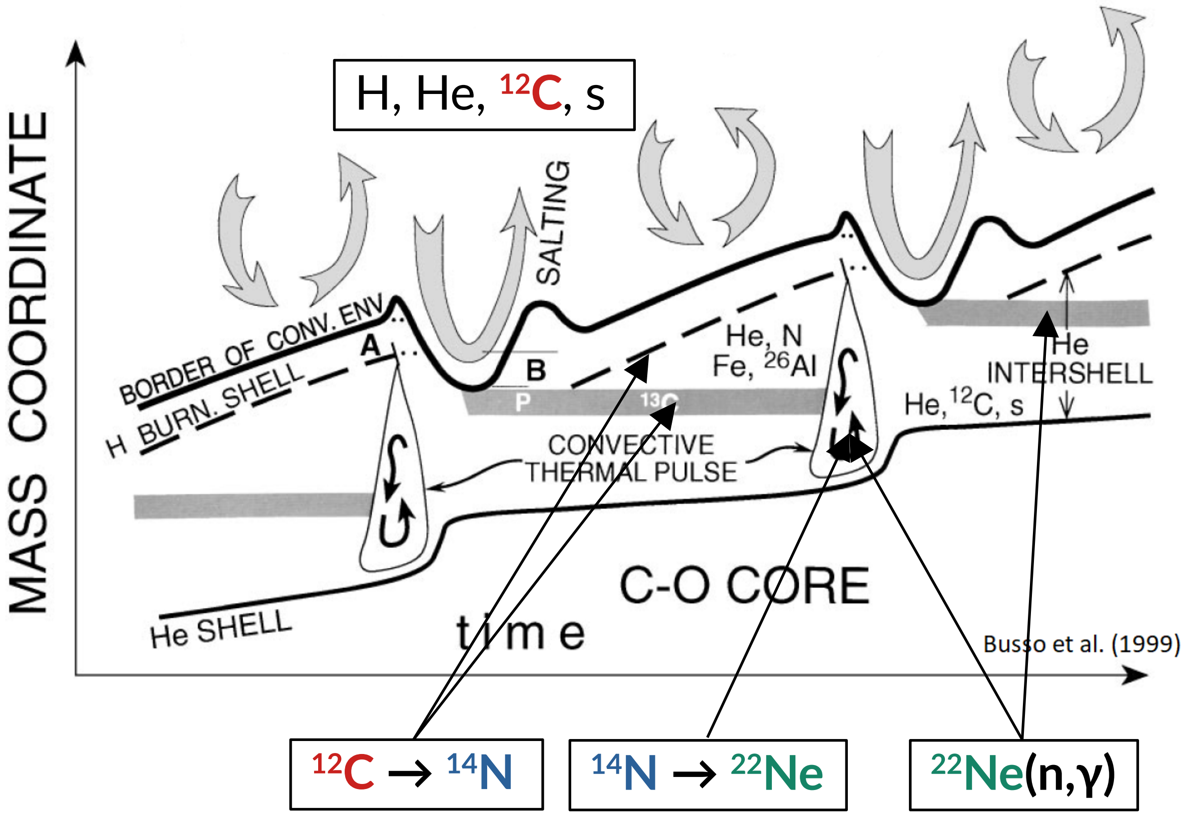

Neutron poisons: the case of ^{22}Ne

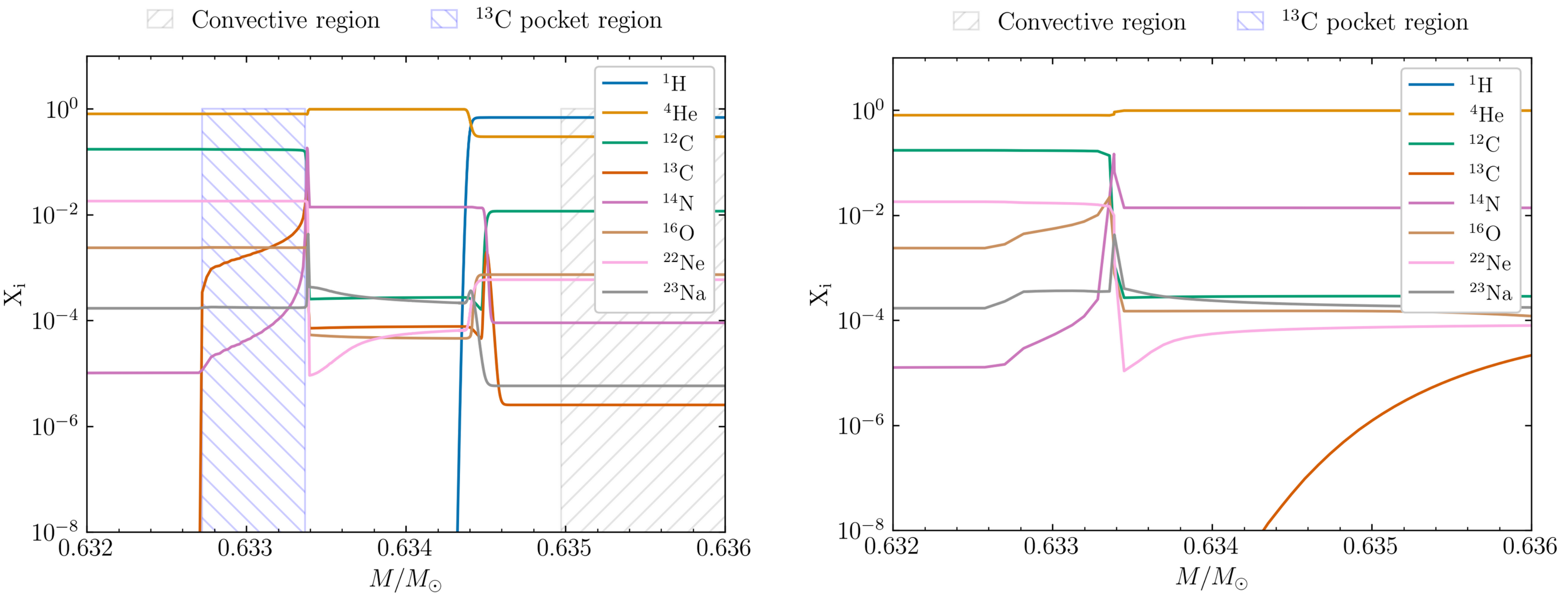

Neutron poisons: the case of ^{22}Ne

- **REF: Bao+ 00**
- **NEW: Heil+ 14**
  - Experimental MACS values of ^{22}Ne for kT = 25 and 52 keV from the activation measurements of Beer+ 91,02
  - Constraints for the relative contributions from dominant DRC and from the resonances at higher energies
  - The p-wave part of the DRC channel contributes significantly at higher energies
  - The s-wave component is defined by the thermal point and the MACS at kT = 25 keV
  - New values are systematically lower up to a **factor of 2** at low energies

➔ **Need for experimental MACS at 5-10keV**